

Calibration of a two-color soft x-ray diagnostic for electron temperature measurement

L. M. Reusch, D. J. Den Hartog, P. Franz, J. Goetz, M. B. McGarry, and H. D. Stephens

Citation: *Rev. Sci. Instrum.* **87**, 11E332 (2016); doi: 10.1063/1.4961281

View online: <http://dx.doi.org/10.1063/1.4961281>

View Table of Contents: <http://aip.scitation.org/toc/rsi/87/11>

Published by the [American Institute of Physics](#)



Calibration of a two-color soft x-ray diagnostic for electron temperature measurement

L. M. Reusch,^{1,a)} D. J. Den Hartog,¹ P. Franz,² J. Goetz,¹ M. B. McGarry,¹ and H. D. Stephens^{1,3}

¹University of Wisconsin - Madison, Madison, Wisconsin 53703, USA

²Consorzio RFX, Padova, Italy

³Pierce College Fort Steilacoom, Lakewood, Washington 98498, USA

(Presented 8 June 2016; received 3 June 2016; accepted 2 August 2016; published online 23 August 2016)

The two-color soft x-ray (SXR) tomography diagnostic on the Madison Symmetric Torus is capable of making electron temperature measurements via the double-filter technique; however, there has been a 15% systematic discrepancy between the SXR double-filter (SXR_{DF}) temperature and Thomson scattering (TS) temperature. Here we discuss calibration of the Be filters used in the SXR_{DF} measurement using empirical measurements of the transmission function versus energy at the BESSY II electron storage ring, electron microprobe analysis of filter contaminants, and measurement of the effective density. The calibration does not account for the TS and SXR_{DF} discrepancy, and evidence from experiments indicates that this discrepancy is due to physics missing from the SXR_{DF} analysis rather than instrumentation effects. *Published by AIP Publishing.* [<http://dx.doi.org/10.1063/1.4961281>]

I. INTRODUCTION

The Madison Symmetric Torus is equipped with a two-color soft x-ray (SXR) tomography diagnostic that has 40 unique and overlapping viewing chords distributed across 4 cameras. Each chord is equipped with two AXUV-1ELM photodetectors that sample the same plasma volume. One has a 427 μm beryllium filter and the other has a 801 μm beryllium filter. Each filter is typically made of a stack of Be foils that are each nominally 80 μm thick. For example, the 427 μm Be filter is a stack of 5 foils. A full description of the diagnostic can be found in Refs. 1 and 2.

The two-color tomography system makes electron temperature (T_e) measurements via the double-filter (SXR_{DF}) technique.^{3,4} SXR_{DF} uses a ratio from detectors with two different thickness filters that share a line of sight to form a coarse spectrometer and estimate the slope of the spectrum, which is temperature dependent. This method relies on the absence of any non-continuum sources of x-ray radiation in the filter passbands (steps in the recombination spectrum or atomic lines) for accurate results. Additionally, the relationship between the ratio and T_e relies on accurate accounting of instrumentation effects.

To that end, a sophisticated model of the SXR tomography system is used to generate predicted ratio values for a specified T_e . The model generates a 2-dimensional x-ray emissivity for specified plasma parameters. In addition to T_e profiles, the model takes electron and impurity density profiles; however, those parameters do not affect the ratio, so the impurities

densities are set to zero (i.e., $Z_{\text{eff}} = 1$) and we use an ansatz profile for the electron density. The model then calculates the line-integrated brightness using experimental lines of sight for each detector, and modeled Be filter and Si photo-detector responses.

Temperatures from SXR_{DF} have been persistently and systematically $\sim 15\%$ lower than Thomson scattering (TS), possibly indicating that not all instrumentation effects have adequately been included in the SXR model. Analysis of geometric effects of the lines of sight as well as the impact of the Al frames used to hold the Si detectors each resulted in a 1%-2% change in brightness, but do not strongly impact the SXR_{DF} T_e .⁵ Initial analysis of contamination in the Be filters suggested that impurities in the filter changed the transmission curve, thus changing the inferred T_e .⁶ In this paper, we present a calibration of the Be filters and the effect on the SXR_{DF} T_e .

II. CALIBRATION MEASUREMENTS

Transmission functions for two Be filters were measured as the basis for the calibration. Measurements were performed by the Physikalisch-Technische Bundesanstalt (PTB) radiometry laboratory⁷ using the four-crystal monochromator (FCM) beamline⁸ at the electron storage ring BESSY II. In order to avoid down-time of the SXR tomography system, the filters sent to PTB were not the same as those used in experiment. Specifically, the filters measured were 348 μm and 702 μm , as opposed to 427 μm and 801 μm . The filters were mounted in the UHV-reflectometer,⁹ and a photodiode was used to detect the transmitted radiation. The diode current was normalized to the stored current in BESSY II to account for a decay in the stored electron current. The dark current of the diode was subtracted, and measurements without filters were taken at each energy before and after filter measurements to account

Note: Contributed paper, published as part of the Proceedings of the 21st Topical Conference on High-Temperature Plasma Diagnostics, Madison, Wisconsin, USA, June 2016.

^{a)}lmmcguire@wisc.edu

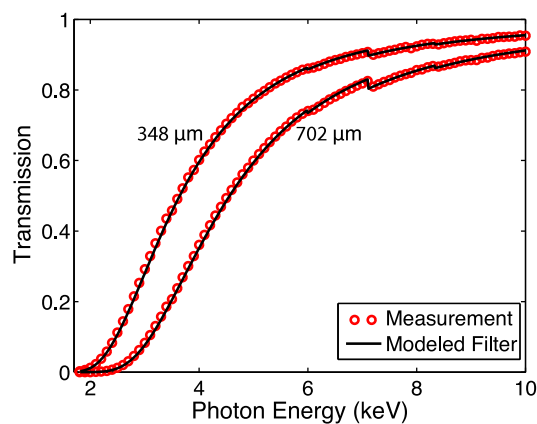


FIG. 1. Open circles (red online) show measured transmission as a function of energy. Absorption edges at 6 keV, 7 keV, and 8.5 keV indicate the presence of Cr, Fe, and Ni, respectively. The solid black curve shows the modeled transmission of impure Be filters containing those same three contaminants.

for the spectral response of the diode and any drift in beam position. The beam had a width of ~ 0.4 mm. Transmission was measured for photon energies between 1.8 keV and 10 keV in steps of 0.1 keV. Results are shown in Fig. 1 as the circles (red online). The measured transmission for both filters shows clear evidence of iron, chromium, and nickel contaminants. These contaminants are consistent with stainless steel equipment used in processing the foils.

Several likely contaminants of the Be filters were quantified using wavelength dispersive electron probe microanalysis (EPMA) with a CAMECA SX51 at the University of Wisconsin-Madison Department of Geoscience.¹⁰ Multiple measurements were made on a grid of 54 points over a $4 \text{ mm} \times 4 \text{ mm}$ area of the foil. The EMPA beam was operated at 25 keV, 25 nA, using a $30 \text{ }\mu\text{m}$ (defocused) beam, and had a detection threshold of 10 ppm. Results in terms of number ratio of atoms are presented in Table I.

The processing of the foils likely causes defects that change the effective density. To accurately account for that, the effective density of the foils was measured by making high precision measurements of the weight and volume of representative foils. The foils measured are the same foils that were calibrated at the PTB. Each foil was imaged on a background with a calibrated $1 \text{ mm} \times 1 \text{ mm}$ grid. The image was digitally enlarged, and the grid was used to find the scale factor. Lengths and widths of the foils were measured to less than 0.1 mm precision. The exact thickness of each foil was measured to a precision of $\pm 1 \text{ }\mu\text{m}$ using a micrometer. An average thickness for each foil was obtained by measuring

TABLE I. Electron probe microanalysis of likely contaminants in Be foils in number ratio of atoms.

Element	EMPA (ppm)	Element	EMPA (ppm)
Zr	Below detection	Ca	40 ± 32
Al	80 ± 26	Cr	20 ± 8
Si	90 ± 32	Fe	190 ± 105
K	Below detection		

three times. The weight of each foil was obtained using a Chainomatic scale (Christian Becker, Inc.) to a precision of 0.1 mg. Again, the foils were measured at least 3 times and the values were averaged. The density of the foils was found to be $1.67 \pm 0.021 \text{ g/cm}^3$. This value differs from the nominal density of Be crystal (1.848 g/cm^3) by approximately 10%. The uncertainty represents both variation in the density from foil to foil as well as the measurement uncertainty.

In order to extrapolate the measured transmission to the thickness used in experiment, the transmission function was modeled using an x-ray filter model. The model uses tabulated measurements of the mass coefficients¹¹ for Be and any contaminants included in the model, the measured effective density of the Be filters, and the measured thickness of each filter. The actual amount of any given contaminant can be used as a fitting parameter. The absorption edges for Cr (at ~ 6 keV), Fe (~ 7 keV), and Ni (~ 8.5 keV) in particular provide strong constraints on the amount of those contaminants. The lack of any strong feature around 4 keV, where the absorption edge for Ca should be, likewise provides a constraint on Ca. The black solid curve in Fig. 1 shows modeled transmission using only Cr (40 ppm), Fe (130 ppm), and Ni (40 ppm) as contaminants in the filter. While EPMA measurements of contaminants in the filters do indicate the presence of other contaminants, those contaminants do not appear to have a strong impact on the transmission.

Excellent agreement between the measured transmission and a numerical model of the filter gives us confidence that we are properly taking into account the important characteristics of the filter. It should be emphasized that the only fitting parameters used to model the transmission function were the contaminant densities; the material density, thickness, and mass coefficients all come from empirical measurements. Also note that the only parameter that differs between the model for the $348 \text{ }\mu\text{m}$ filter and the $702 \text{ }\mu\text{m}$ filter is the thickness. We conclude that we have fully characterized the foils. Furthermore, we have characterized them using a technique that allows the calibration information to be applied to any thickness filter desired simply by changing the specified thickness in the filter model.

III. EFFECT ON T_e

Using the calibration information results in a small change in the ratio curves used to infer the electron temperature, resulting in a very small change to the $\text{SXR}_{\text{DF}} T_e$. This is illustrated in Fig. 2 which shows that the $R(T_e)$ using a 100% pure Be foil (solid curve (red online)) is nearly same as the $R(T_e)$ using a calibrated filter (dashed curve (black)). Figure 3 shows the percent discrepancy between temperatures from SXR_{DF} and TS, defined as $\frac{(TS - \text{SXR}_{\text{DF}}) * 100}{TS}$, plotted versus T_e from TS when using the calibrated filter model. The discrepancy for a 100% pure Be filter is $\sim 13\%$, and the discrepancy when using a fully calibrated filter is $\sim 15\%$.

Accounting for the effective density of the Be filters as well as the contaminants presents full calibration of the Be filters used in the SXR_{DF} system. The accuracy of the $\text{SXR}_{\text{DF}} T_e$ is increased; however, there is still a 15%

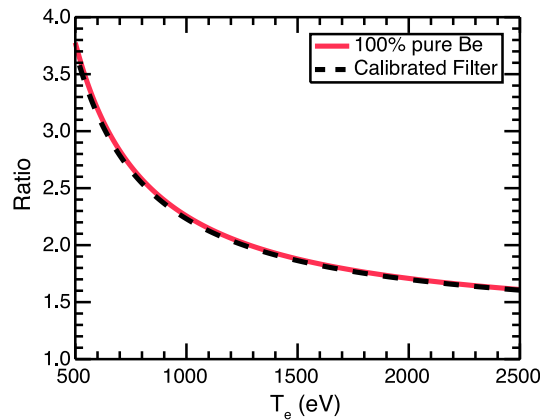


FIG. 2. Tabulated ratio value as a function of input T_e for pure Be filters (solid, red online) and calibrated filters (dashed, black).

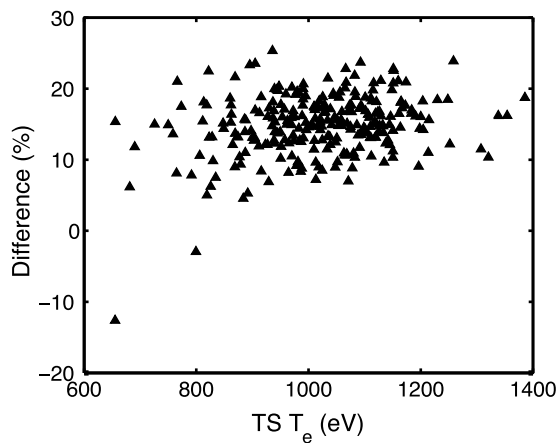


FIG. 3. Percent discrepancy between T_e from SXR_{DF} (using calibrated filters) and TS versus T_e from TS for a distribution of temperatures.

disagreement between TS and SXR_{DF}. We have accounted for geometric and instrumentation effects; we strongly suspect that this disagreement is due to non-continuum x-ray emission contaminating the measurements.

Aluminum impurities are present in the MST plasmas due to an Al first wall. Al_{KII} has a principal transition at 1600 eV and Al_{KIII} has a principal transition at 1730 eV. These lines radiate very strongly, so while the transmission through a 427 μm filter for the line energies is around 10^{-5} , it is possible that enough radiation is transmitted to affect the SXR_{DF} temperature. Evidence for this has been seen in experiments where one camera of the SXR system had a 427/801 μm pair and another camera had a 583/833 μm pair. Figure 4 shows the discrepancy for the two sets of filters. As before, the 427/801 μm filters have a $\sim 15\%$ discrepancy from TS; however, when using a thicker pair of filters, 583/833 μm , the mean discrepancy is less than 2%. This is likely because the 583 μm filter better more effectively filters out Al radiation lines. In principle this pair of filters provides a more reliable temperature measurement; however, the use of these thicknesses restricts T_e measurements to high

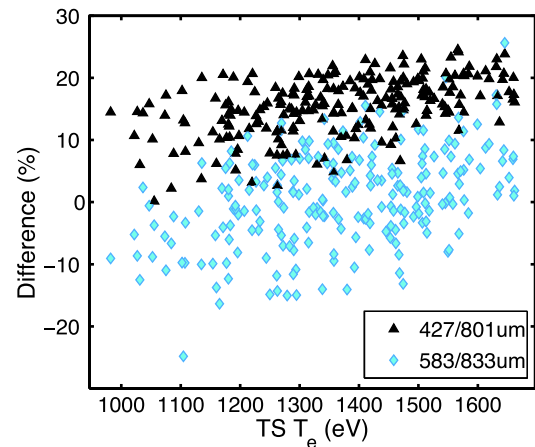


FIG. 4. Percent discrepancy between T_e from SXR_{DF} and TS versus TS for a 427/801 μm pair of filters (triangles, black) compared to a 583/833 μm pair of filters (diamonds, cyan online). Calibrated filters were used in the analysis for both pairs.

temperatures. Additionally, the ratio curve is relatively flat, reducing sensitivity in the T_e range of interest. Future work will concentrate on verifying that line radiation is indeed the cause of the discrepancy between SXR_{DF} and TS, and, if so, quantifying it in order to accurately include it in the SXR_{DF} analysis. MST data shown in this paper can be obtained in digital format at the [supplementary material](#).

SUPPLEMENTARY MATERIAL

See [supplementary material](#) to obtain the digital format for the data shown Figs. 1–4.

ACKNOWLEDGMENTS

This material is based upon work supported by the U.S. Department of Energy, Office of Science, Office of Fusion Energy Sciences under Award No. DE-FC02-05ER54814.

- ¹M. B. McGarry, P. Franz, D. J. Den Hartog, and J. A. Goetz, *Rev. Sci. Instrum.* **81**, 10E516 (2010).
- ²M. B. McGarry, P. Franz, D. J. Den Hartog, J. A. Goetz, M. A. Thomas, M. Reyfman, and S. T. A. Kumar, *Rev. Sci. Instrum.* **83**, 10E129 (2012).
- ³F. C. Jahoda, E. M. Little, W. E. Quinn, G. A. Sawyer, and T. F. Stratton, *Phys. Rev.* **119**, 843 (1960).
- ⁴T. P. Donaldson, *Plasma Phys.* **20**, 1279 (1978).
- ⁵M. B. McGarry, P. Franz, D. J. Den Hartog, J. A. Goetz, and J. Johnson, *Rev. Sci. Instrum.* **85**, 096105 (2014).
- ⁶M. B. McGarry, P. Franz, D. J. D. Hartog, and J. A. Goetz, *Plasma Phys. Controlled Fusion* **56**, 125018 (2014).
- ⁷B. Beckhoff, A. Gottwald, R. Klein, M. Krumrey, R. Miller, M. Richter, F. Scholze, R. Thornagel, and G. Ulm, *Phys. Status Solidi B* **246**, 1415 (2009).
- ⁸M. Krumrey and G. Ulm, *Nucl. Instrum. Methods Phys. Res., Sect. A* **467-468**, 1175 (2001).
- ⁹D. Fuchs, M. Krumrey, F. Scholze, and G. Ulm, *Rev. Sci. Instrum.* **66**, 2248 (1995).
- ¹⁰S. J. B. Reed, *Electron Microprobe Analysis*, 2nd ed. (Cambridge University Press, Cambridge, 1993), p. 326.
- ¹¹E. Gullikson *et al.*, “X-ray properties of the elements,” http://henke.lbl.gov/optical_constants/pert_form.html.